

Inverted Pendulum System Disturbance and Uncertainty Effects Reduction using Sliding Mode-Based Control Design

Nagy Osman
Higher Colleges of Technology,
Department of Electrical
Engineering, Sharjah, UAE. Email:
nosman@hct.ac.ae

Haris M. Khalid, SM IEEE,
Higher Colleges of Technology,
Department of Electrical
Engineering, Sharjah, UAE. Email:
harism.khalid@yahoo.com

Raouf Fareh
University of Sharjah, Department
of Electrical Engineering, Sharjah,
UAE, Email: rfareh@sharjah.ac.ae

Jawher Ghommam
Sultan Qaboos University,
Department of Electrical and
Computer Engineering, Sultanate of
Oman, Email: jawher@squ.edu.om

Tha'er O Sweidan
Higher Colleges of Technology,
Department of Electrical
Engineering, Sharjah, UAE. Email:
tsweidan@hct.ac.ae

Abstract— The system behavior of a dual-axis inverted pendulum in the presence of parametric uncertainty could be very challenging from the perspective of control handling. It becomes more challenging in the presence of model uncertainties, external disturbances and chattering phenomenon. In this paper, a sliding mode-based control design is proposed to handle the dynamics, system disturbances and uncertainty effects of an inverted pendulum. This is achieved by: a) approximating the discontinuity in the control law, b) handling the origin of chatter effect by using a continuous function, and c) Euler method with small step size. Simulation results show that the sliding mode controller in the presence of disturbance can eliminate the chattering phenomenon, improve the control precision, and suppress the effects of external disturbance and model uncertainties effectively.

Keywords— dynamics modelling, inverted pendulum, linear quadratic regulator (LQR), parametric uncertainty, proportional integral derivative (PID), sliding mode control (SMC).

I. INTRODUCTION

The stability of an inverted pendulum is crucial and has attracted many control researchers and experts since last many years. This is due to its complex and non-linear structure with a high order, unstable system dynamics, and under-actuated more degrees of freedoms than the number of control inputs [1]–[2]. It is due to this reason that inverted pendulum are vastly discussed in control and stability design applications. This ranges from balancing robots and vehicles [3]–[6] to humanoid robots [7]–[8], oscillator synchronization [9]–[10], etc. Moreover, most of the applications are also commercialized with ready-to-use lab-based experiments and other educational assets, such as the Pendulum and Cart Control Systems [11], the Ball with Pendulum suspension system [12], and rotary inverted pendulum [13] can be indicated. These applications focus on several dynamics such as nonlinearity, rational, single-joint and multi-joint systems. This makes the practical applications of the inverted pendulum and its study even more interesting and important. This may lead to other advance applications as well which consider the extended dynamics of inverted pendulum, such as rockets, guided missiles, and intelligent robots. The main focus of this work is on the linear single joint inverted pendulum and its related dynamics.

The main challenge towards systems stability and control of an inverted pendulum is its swinging position against gravitational forces while maintaining the equilibrium point. In this regard, the inverted pendulum system stability problem first solution was introduced mechanically in 1960 by Roberge, J. K. [14]. Researchers consequentially considered this problem and various control systems are implemented to achieve the system stability. Traditional controllers are applied like PID controller and various configurations [15]–[17]. However, it was not that efficient to control such complex systems. It is because it was not able to handle system uncertainty and unpredictable disturbances adequately [18]. The robustness of the system decreases with parametric and structural uncertainties consequently while making tuning of gains in PID control laws [19]. These challenges highlight the role of more advanced and sophisticated control strategies like State feedback control [20] and Linear Quadratic Regulator (LQR) [21] or its variants, which can provide a systematic way to accurately track the desired trajectories. However, both techniques and their variants were not efficient with the complex systems in the presence of uncertainties and disturbances, which is the main motivation of this paper.

The contribution of this paper is to derive a sliding mode-based control design which could handle the instability problem of the inverted pendulum in the presence of disturbances. This is specially required in situations where the certain parameters are not known and require observability. The sliding mode-based control design was able to handle these dynamics. Forces summation were developed for both cart and the pendulum. A set of governing equations were derived on top of these summation forces. To handle the parametric uncertainty, a tool for small angle approximation was utilized. This was further supported by the approximating function of control law and handling the chattering phenomenon for any external disturbances.

The formation of rest of the paper is built as follows: Section II represents the problem formulation of the proposed system. The implementation and evaluation of the proposed scheme is described in Section III. Finally, conclusions are drawn in Section IV.

II. PROBLEM FORMULATION – INVERTED PENDULUM SYSTEM DISTURBANCE AND UNCERTAINTY EFFECTS REDUCTION

The problem formulation of the inverted pendulum is derived in this section. An overview of framework is illustrated in Fig. 1. The system model comprises of an inverted pendulum mounted to a motorized cart. The inverted pendulum system is an example commonly found in control system textbooks and research literature. Its popularity derives in part from the fact it is unstable without control. This means that the pendulum simply falls over if the cart does not move to balance it. Additionally, the dynamics of the system are nonlinear. The objective of the control system is to balance the inverted pendulum by applying a force to the cart that the pendulum is attached to. A real-world example that relates directly to this inverted pendulum system is the attitude control of a booster rocket at takeoff. Fig. 1 summarizes the steps involved in problem formulation as follows: The problem formulation begins with the forces of the cart (1) and pendulum (2) in the horizontal direction. This is followed by first (3)--(5) and second governing equations (6) respectively. The small angle approximation and governing equation is introduced in (7)--(10). The transfer function of the linearized system equation is derived in (11)--(16). The system state space model is represented in (17)--(25).

A. Inverted Pendulum – System Dynamics and Equations of Motion

Consider a two-dimensional problem in Fig. 1, where the pendulum is constrained to move in the vertical plane shown in the figure below. For this system, the control input is the force F that moves the cart horizontally and the outputs are the angular position of the pendulum θ and the horizontal position of the cart x . M is the mass of cart, m is the mass of pendulum rod, L is the length of pendulum where $l = L/2$, and $I = 1/3 ml^2$.

A.1. Forces Summation of the Cart in Horizontal Direction: Summing the forces in the free-body diagram of the cart in the horizontal direction, the equation of motion would be as follows:

$$M\ddot{x} + b\dot{x} + N = F \quad (1)$$

Note the forces can be summed in the vertical direction for the cart as well. However, no useful information would be gained from that summation.

A.2. Forces Summation of the Pendulum in Horizontal Direction: Summing the forces in the free-body diagram of the pendulum in the horizontal direction, the expression for the reaction force N would be as:

$$N = m\ddot{x} + ml\ddot{\theta}\cos\theta - ml\dot{\theta}^2\sin\theta \quad (2)$$

A.3 First Governing Equation: Substituting (2) in (1) gives the following first governing equation for the system as:

$$(m + M)\ddot{x} + b\dot{x} + ml\ddot{\theta}\cos\theta - ml\dot{\theta}^2\sin\theta = F \quad (3)$$

To get the second equation of motion for this system, sum the forces perpendicular to the pendulum. Solving the

system along this axis greatly simplifies the mathematics. This would eventually give the following equation:

$$N\cos\theta - P\sin\theta - mg\sin\theta = ml\ddot{\theta} + M\ddot{x}\cos\theta \quad (4)$$

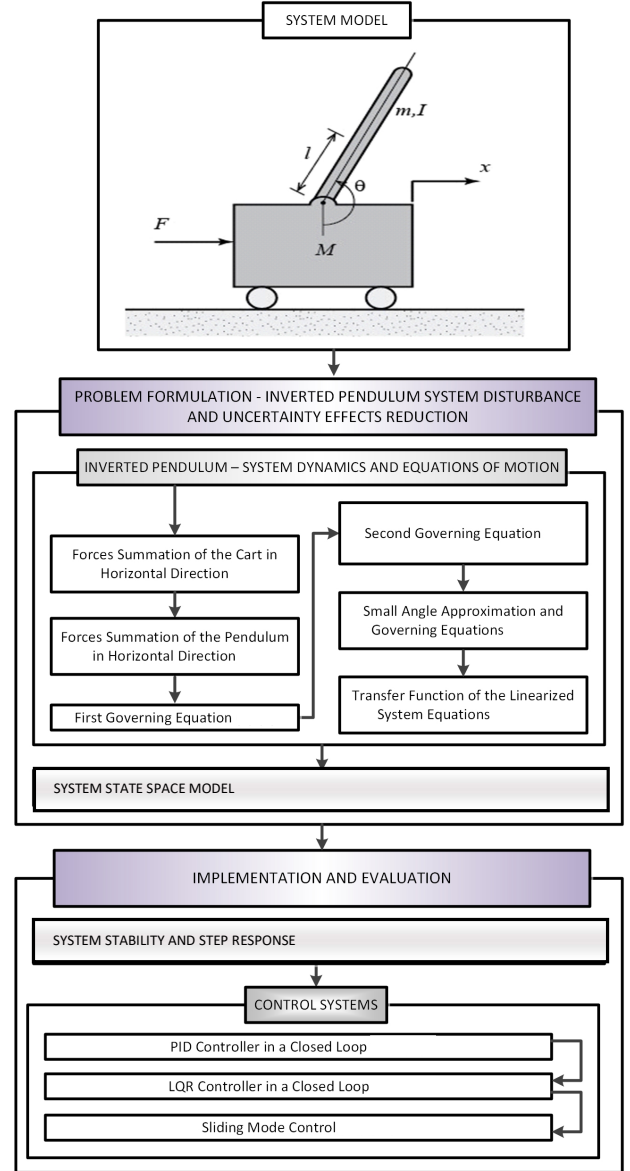


Figure. 1 Proposed Scheme for System Disturbance and Uncertainty Effects Reduction of Inverted Pendulum

Sum up the moments along the centroid of the pendulum and get rid of the P and N terms in (4) to conclude the following equation..

$$-Pl\sin\theta + Nl\cos\theta = I\ddot{\theta} \quad (5)$$

A.4. Second Governing Equation: Combining the last two expressions, the second governing equation is achieved as follows:

$$(I + ml^2)\ddot{\theta} + mglsin\theta = ml\ddot{x}\cos\theta \quad (6)$$

Since the considered analysis and control design techniques are applied to the linear model, this set of equations is required to be linearized.

A.5. Small Angle Approximation and Governing Equations: The equations about the vertically upward equilibrium position are linearized, $\theta = \pi$, and will assume that the system stays within a small neighborhood of this equilibrium. This assumption should be reasonably valid since under control it is desired that the pendulum should not deviate more than 20 degrees from the vertically upward position. Let ϕ represent the deviation of the pendulum's position from equilibrium, that is, $\theta = \pi + \phi$. Again, presuming a small deviation (ϕ) from equilibrium, the following small angle approximations of the nonlinear functions in system equations is used:

$$\cos\theta = \cos(\pi + \phi) \approx -1 \quad (7)$$

$$\sin\theta = \sin(\pi + \phi) \approx -\phi \quad (8)$$

After substituting the above approximations into the nonlinear governing equations, it gives the two linearized equations of motion. Note it has been substituted for the input F .

$$(I + ml^2)\ddot{\phi} - mgl\sin\phi = ml\ddot{x} \quad (9)$$

$$(m + M)\ddot{x} + b\dot{x} + ml\ddot{\phi} = u \quad (10)$$

where u is the input force F

A.6 Transfer Function of the Linearized System Equations: To obtain the transfer functions of the linearized system equations, it is required to first take the Laplace transform of the system equations assuming zero initial conditions. The resulting Laplace transforms are shown below:

$$(I + ml^2)\phi(s)s^2 - mgl\sin\phi(s) = mlx(s)s^2 \quad (11)$$

$$(m + M)x(s)s^2 + bx(s)s + ml\phi(s)s^2 - U(s) \quad (12)$$

Since a transfer function represents the relationship between a single input and a single output at a time, $X(s)$ is required to be eliminated for the first transfer function for the output $\phi(s)$ and an input of $U(s)$. Solve the first equation for (s) .

$$X(s) = \left[\frac{I + ml^2}{ml} - \frac{g}{s^2} \right] \phi(s) \quad (13)$$

Then substitute the above into the second equation gives:

$$(M + m) \left[\frac{I + ml^2}{ml} - \frac{g}{s^2} \right] \phi(s)s^2 + b \left[\frac{I + ml^2}{ml} - \frac{g}{s^2} \right] \phi(s)s - ml\phi(s)s^2 = U(s) \quad (4)$$

Rearranging, the transfer function is then the following:

$$\frac{\phi(s)}{U(s)} = \frac{\frac{ml}{q} s^2}{s^4 + \frac{b(I + ml^2)}{q} s^3 - \frac{(M + m)mgl}{q} s^2 - \frac{bmgl}{q} s} \quad (14)$$

where $q = (M + m)(I + ml^2) - ml^2$

From the transfer function above there is both a pole and a zero at the origin. These can be canceled, and the transfer

function becomes the following (which is called the pendulum angle transfer function).

$$\frac{\phi(s)}{U(s)} = \frac{\frac{ml}{q} s}{s^3 + \frac{b(I + ml^2)}{q} s^2 - \frac{(M + m)mgl}{q} s - \frac{bmgl}{q}} \quad (15)$$

second, the transfer function with the cart position (s) as the output can be derived in a similar manner to arrive at the following:

$$\frac{X(s)}{U(s)} = \frac{\frac{(I + ml^2)s^2 - mgl}{q}}{s^4 + \frac{b(I + ml^2)}{q} s^3 - \frac{(M + m)mgl}{q} s^2 - \frac{bmgl}{q} s} \quad (16)$$

2.1 System State Space Model

Assume x_1, x_2, x_3, x_4 are the system states and $x_1 = x, x_2 = \dot{x}, x_3 = \ddot{x}, x_4 = \ddot{\phi}$ and $\dot{x}_1 = \dot{x}$, then substitute into Eq. (9)-(10):

$$(M + m) \dot{x}_2 + bx_2 - ml \dot{x}_4 = u \quad (17)$$

$$(I + ml^2) \dot{x}_4 + mglx_3 = ml\dot{x}_2 \quad (18)$$

Now substitute value of \dot{x}_4 gives:

$$\begin{aligned} \dot{x}_2 &= \ddot{x} = -\frac{b(I + ml^2)}{q} x_2 + \frac{m^2 g l^2}{q} x_3 + \\ \frac{(I + ml^2)}{q} u &= -\frac{b(I + ml^2)}{q} \dot{x} + \frac{m^2 g l^2}{q} \ddot{\phi} + \\ \frac{(I + ml^2)}{q} u & \end{aligned} \quad (19)$$

And substitute value of \dot{x}_2 gives:

$$\begin{aligned} \dot{x}_4 &= \ddot{\phi} = -\frac{bml}{q} x_2 + \frac{(M + m)mgl}{q} x_3 + \\ \frac{ml}{q} u &= -\frac{bml}{q} \dot{x} + \frac{(M + m)mgl}{q} \ddot{\phi} + \frac{ml}{q} u \end{aligned} \quad (20)$$

The matrices A, B and C can be derived as follows:

$$A = \begin{bmatrix} 0 & 1 & 0 & 0 \\ 0 & -\frac{b(I + ml^2)}{I(M + m) - Mml^2} & \frac{m^2 g l^2}{I(M + m) - Mml^2} & 1 \\ 0 & -\frac{bml}{I(M + m) - Mml^2} & \frac{(M + m)mgl}{I(M + m) - Mml^2} & 0 \\ 0 & 0 & 0 & 0 \end{bmatrix} \quad (21)$$

$$B = \begin{bmatrix} 0 \\ \frac{(I + ml^2)}{I(M + m) - Mml^2} \\ 0 \\ ml \end{bmatrix} \quad (22)$$

$$C = \begin{bmatrix} 1 & 0 & 0 & 0 \\ 0 & 1 & 0 & 0 \end{bmatrix} \quad (23)$$

Finally the system state space model including four states ($\dot{x}, \ddot{x}, \ddot{\phi}, \ddot{\phi}$), in which those states are: a) cart velocity, b) cart acceleration, c) pendulum angular velocity, and d) angular acceleration respectively. Moreover, it has two outputs: 1) cart position, and 2) pendulum angle. And one

input: 1) the force applied to the system. The state space model presented as shown below:

$$\begin{bmatrix} \dot{x} \\ \dot{x} \\ \dot{\phi} \\ \dot{\phi} \end{bmatrix} = \begin{bmatrix} 0 & 1 & 0 & 0 \\ -\frac{b(I+ml^2)}{I(M+m)-Mml^2} & -\frac{m^2gl^2}{I(M+m)-Mml^2} & 0 & 0 \\ 0 & \frac{bml}{I(M+m)-Mml^2} & \frac{(M+m)mgI}{I(M+m)-Mml^2} & 0 \\ 0 & 0 & 0 & 0 \end{bmatrix} \begin{bmatrix} x \\ \dot{x} \\ \phi \\ \dot{\phi} \end{bmatrix} + \begin{bmatrix} 0 \\ \frac{I(M+m)-Mml^2}{I(M+m)-Mml^2} \\ 0 \\ \frac{ml}{I(M+m)-Mml^2} \end{bmatrix} u \quad (24)$$

$$y = \begin{bmatrix} 1 & 0 & 0 & 0 \\ 0 & 1 & 0 & 0 \end{bmatrix} \begin{bmatrix} x \\ \dot{x} \\ \phi \\ \dot{\phi} \end{bmatrix} + \begin{bmatrix} 0 \\ 0 \end{bmatrix} u \quad (25)$$

III. IMPLEMENTATION AND EVALUATION

Fig. 1 shows the steps involved in implementation and evaluation of the proposed scheme and control design on the inverted pendulum. The system stability and step response is discussed in (26)--(28). The control is deployed in a closed loop with PID, LQR, and sliding mode control in (29)--(31), (32)--(33), and (34)--(38) respectively.

A. System Stability and Step Response

Stable system have closed-loop transfer functions with poles only in the left half-plane. The system parameters are listed in Table 2. By using the characteristic equation, the poles and poles location can be identified as:

$$\det(SI - A) = 0 \quad (26)$$

$$SI - A = \begin{bmatrix} s & -1 & 0 & 0 \\ 0 & s + \frac{2}{11} & -\frac{147}{55} & 0 \\ 0 & 0 & s & -1 \\ 0 & \frac{5}{11} & -\frac{343}{11} & s \end{bmatrix} \quad (27)$$

$$\det(SI - A) = s^4 + \left(\frac{2}{11}\right)s^3 - \left(\frac{343}{11}\right)s^2 - \left(\frac{49}{11}\right)s = 0 \quad (28)$$

So the system poles are: 0, 5.5651, -5.6041 and -0.1428. It can be seen there is one pool located in the right half plane. It can be seen there is one pool located in the right half plane (RHP) (Positive pool which is 5.5651) as shown in Fig. 2(a). As it can be seen in Fig. 2(b), the system response is entirely unsatisfactory. In fact, it is not stable in open loop. Although the pendulum's position is shown to increase by 50 radians. It is also noticed that the cart position moves infinitely far to the right. So, a proper controller is required to design. When a step reference is given to the system, the pendulum should be displaced but eventually return to the equilibrium position and the cart should move to its new commanded position.

Once the system stability and step response are calculated, control system design is presented to deal with the instability problem of the inverted pendulum in the presence of disturbance.

B. Control Systems

B.1. PID Controller in a Closed Loop: Generating the control system design, a PID controller is placed in a closed-loop unity feedback system as shown in Fig. 2(c). The variable e(t) denotes the tracking error, which is sent to the PID controller.

The PID controller transfer function is given by:

$$C(s) = K_p + K_i \frac{1}{s} + K_d s \quad (29)$$

The pendulum angle transfer function is given by:

$$\frac{\Phi(s)}{F(s)} = \frac{P_{pen}}{1 + C(s)P_{pen}} \quad (30)$$

And the cart position transfer function is given by:

$$\frac{X(s)}{F(s)} = \frac{P_{cart}}{1 + C(s)P_{cart}} \quad (31)$$

To achieve the design requirements which are firstly, the settling time should be less than 5 seconds, rise time for cart position should be less than 0.5 seconds and pendulum angle θ should never exceeds 20 degrees (0.35 radians) from the vertical, tuning the parameter of the PID controller is required as shown in Table. 1. The controller is set for two situations here: a) K_p equal to 50, and b) K_p equal to 50 and K_i equal to 20.

B.1.1 K_p equal to 50: The effect on the system response can be seen by increasing K_p (pendulum angle). The K_p will be set to 50. This gives the system response shown in Fig. 3(a). As shown in the Fig. 3(a), settling time is 1.74s, so it is less than the system requirements. This will not change the integral gain K_i because the steady state error is already approximately equal to zero. It has been also noticed here that the pendulum max angle is approximately 0.25 rad. This will eventually improve the angle by increasing the derivative gain to 20. The system response with the new setting can be seen in Fig. 3(a).

B.1.2 K_p equal to 50, and K_i equal to 20: In this case, K_p is set equal to 50 and K_i equal to 20. The required performance is achieved as can be seen in Fig. 3(b). The maximum pendulum angle is less than 0.05 rad and the settling time is 1.82 sec. But as shown in Fig. 3(c), the cart (position) moves in the negative direction with approximately constant velocity. Therefore, although the PID controller stabilizes the angle of the pendulum, this design would not be feasible to implement on an actual physical system.

C. LQR Controller in a Closed Loop

An attempt is required to keep the pendulum vertical while controlling the cart's position to move 0.2 meters to the right. A state-space design approach is well suited to the control of multiple outputs. This problem can be solved using LQR controller. The schematic of this type of control system is shown Fig. 4(a)-(c) where K is a matrix of control gains. Note that here the feedback of all of the system's states is deployed rather than using the system's outputs for feedback.

C.1. Preliminary Steps before the Controller Implementation: The preliminary steps required before the application of controller are as follows: 1) Check if the system is controllable or not. If the system is satisfactorily controllable, this allows to derive the state of the system in finite time (under the physical constraints of the system). 2)

The controllability matrix must have rank n , where the rank of a matrix is the number of linearly independent rows (or columns). 3) The determinant of the matrix should be not equal to zero. The controllability matrix (U) can be calculated using below formula:

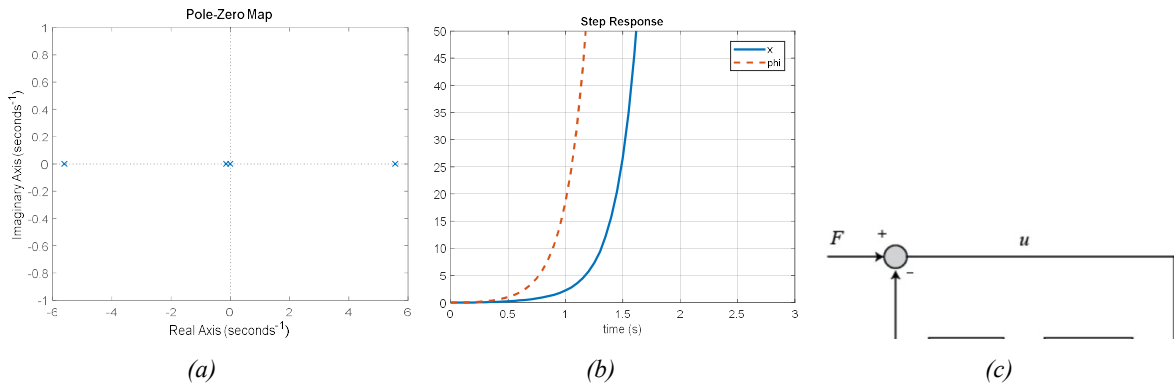


Figure. 2 System stability (a) pole zero map, (b) system step response, (c) system block diagram using PID

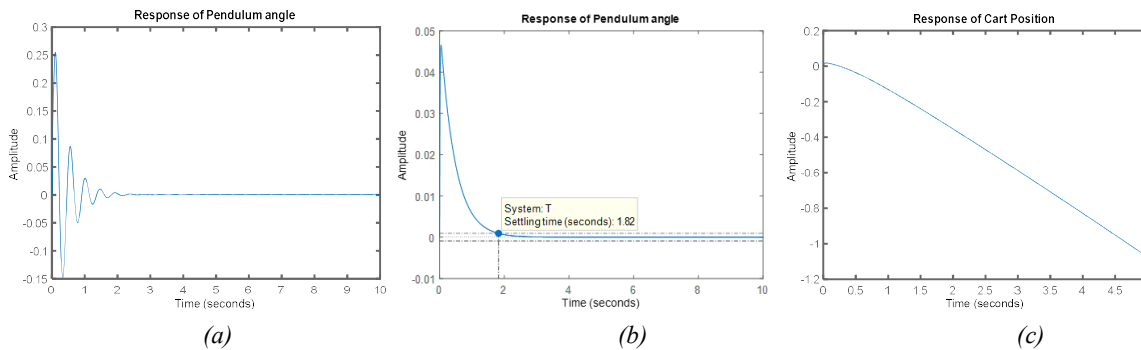


Figure.3 (a) Pendulum angle response with $K_p = 50, K_i = 0$ and $K_D = 0$, (b) Pendulum angle response with $K_p = 50, K_i = 0$ and $K_D = 20$, (c) Cart position response with $K_p = 50, K_i = 0$ and $K_D = 20$

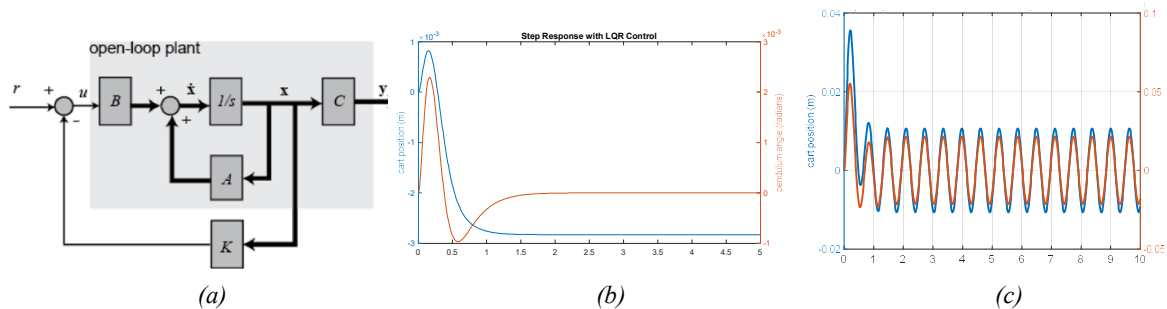


Figure. 4 (a) System block diagram using LQR, System response using (b) LQR, (c) in the presence of disturbances

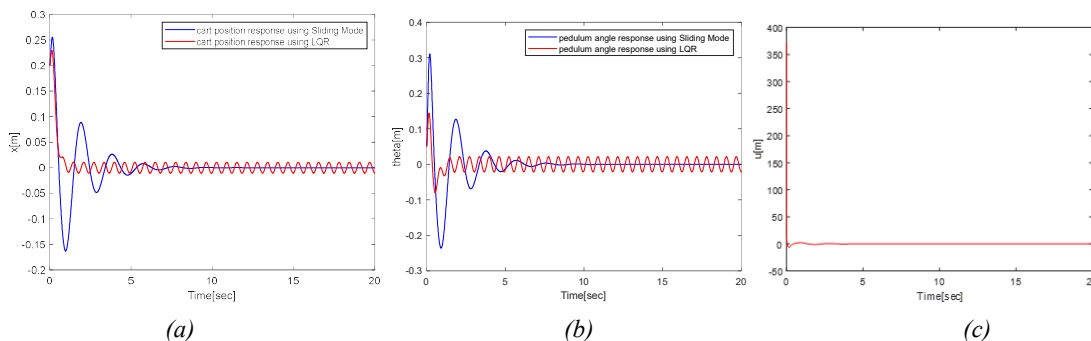


Figure. 5 (a) Cart position, and (b) Pendulum angle response using SMC and LQR, (c) SMC control input

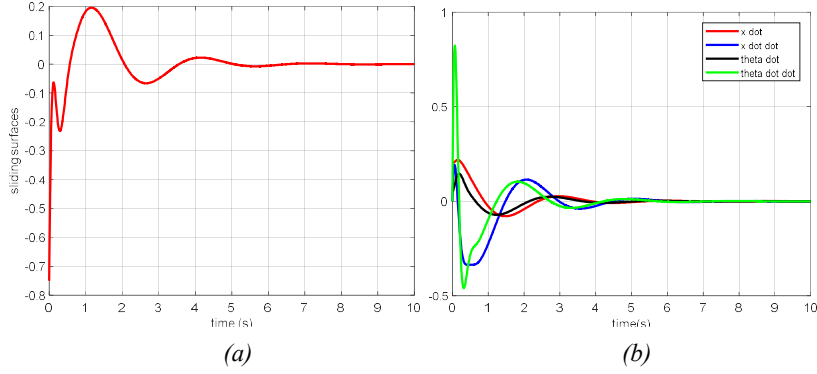


Figure. 6 (a) Sliding surface, and (b) System states

Table 1. Simulation parameters

Parameter increase	Rise time	Overshoot	Settling time	Steady-state error
K_p	Decrease	increase	Small change	Decrease
K_i	Decrease	increase	increase	Great reduce
K_d	Small change	Decrease	Decrease	Small change

$$U = [B \ AB \ A^2B \ \dots \ A^{n-1}B] \quad (32)$$

The rank of the matrix is 4 and determinant is equal to 4.1e04 (which is not zero). So the verified system is completely controllable, now will start to implement linear quadratic regulator (LQR)-based controller.

C.2. LQR Implementation: A performance index J (as shown below) is a mathematical measure of the quality of system behavior. Large J implies poor performance and small J implies good performance.

$$J = \int_0^{mf} (X^T QX + U^T Ru) dt \quad (33)$$

This requires optimizing J to get a good performance and less energy, hence the choices of Q and R allow tradeoffs between performance and energy. Here will use $R = 1$ and $Q = C^T C$ to design an optimal control using LQR and after several trials, will set the Q(1,1) element to be 5000 and Q(3,3) to be 100, the system response shown in Fig. 5(a)-(b).

From Fig. 6(a)-(b), it can be noticed that the rise time and settling time achieved the requirements. Moreover, the pendulum angle and cart position are both stable and achieved the design requirements. LQR controller provide a systematic way to accurately track the desired trajectories, but it is not efficient with the complex systems where uncertainties and disturbances using sinusoidal function are present as shown in Fig. 6(a)-(b).

In the formulation of any practical control problem, there will always be a discrepancy between the actual plant and its mathematical model used for the controller design. These discrepancies (or mismatches) arise from unknown external disturbances, plant parameters, and parasitic/unmolded +

Designing control laws that provide the desired performance to the closed-loop system in the presence of these disturbances/uncertainties is a very challenging task in control engineering. This gives rise to deploy an efficient robust controller (sliding mode control) that provide the desired performance of the closed loop system in the presence of disturbance and uncertainties.

C. Sliding Mode Control (SMC)

The sliding variable is introduced in sliding mode control as shown below:

$$S = f(x_1, x_2, x_3, x_4) = c_1 x_1 + c_2 x_2 + c_3 x_3 + x_4 \quad (34)$$

Where $c_1, c_2, c_3 > 0$

In order to achieve asymptotic convergence of the state variables $x_1(t), x_2(t), x_3(t), x_4(t)$ to zero, i.e., $\lim_{t \rightarrow \infty} x_1, x_2, x_3, x_4 = 0$ and in the presence of the bounded disturbance, $f(x_1, x_2, x_3, x_4, t)$, the variable in Eq. (32)-(33) is derived to zero in finite time by means of the control input (u).

$$\dot{S} = \frac{ds}{dt} = c_1 \dot{x}_1 + c_2 \dot{x}_2 + c_3 \dot{x}_3 + \dot{x}_4 \quad (35)$$

By selecting $\dot{S} = -\tan(s)$ and substitute in Eq. (35)

$$c_1 \dot{x}_1 + c_2 \dot{x}_2 + c_3 \dot{x}_3 + \dot{x}_4 = -\tan(s) \quad (36)$$

Substitute the states (x_1, x_2, x_3, x_4) in Eq. (36) and multiply tan function by constant (ρ) to reduce the shuttering effect

$$\left(c_1 - \frac{b(I + ml^2)}{q} c_2 - \frac{bml}{q} \right) \dot{x} + \left(\frac{m^2 gl^2}{q} c_2 + c_3 \right) \ddot{x} + \left(\frac{(M + m)mgl}{q} \right) \Phi + \left(\frac{(I + ml^2)}{q} + \frac{ml}{q} \right) u = -\rho \tan(s) \quad (37)$$

Finally, the control input u can be determine as in Eq. (37):

$$u \left(\frac{(I + ml^2)}{q} + \frac{ml}{q} \right) = - \left(c_1 - \frac{b(I + ml^2)}{q} c_2 - \frac{bml}{q} \right) \dot{x} - \left(\frac{m^2 gl^2}{q} c_2 + c_3 + \frac{(M + m)mgl}{q} \right) \Phi - \rho \tan(s) \quad (38)$$

D. Results and Discussions

The simulations involved in the proposed work were performed on MATLAB and tools. Then sliding mode controller is designed and incorporated to it. Following are the plant and controller parameter are listed in Table 2

Table 2. System parameters

Parameter	Value
(M) mass of cart	0.5 kg
(m) mass of pendulum	0.2 kg
(b) friction coefficient of cart	0.1 N/m/sec
(l) length to pendulum center of mass	0.3 m
(I) pendulum mass moment of inertia	0.006 kg.m ²

Initial conditions of the cart and pendulum are $(\mathbf{x}, \dot{\mathbf{x}}) = (0.2, 0)$, $(\Phi, \dot{\Phi}) = (0.05, 0)$ and the desired position are set as $y_d = 2$, $\theta_d = 0$ and $y'_d = \theta'_d = 0$. Simulations are done using: $\rho = 7$ and $c_1 = -9$ for the SMC, $c_2 = 2$ and $c_3 = 5$.

In Fig. 5(a)-(b), simulation results for the two controllers have been done. The convergence of state variables has been established for all controllers.

Furthermore, system states for SMC controller converge faster than LQR. It has also been noticed that there is a robust behavior of the SMC controllers with respect to parametric uncertainties (disturbance). Also, it can be observed that by using Euler method with small step size, SMC is able to effectively compensate the chattering phenomenon.

Fig. 5(c) and Fig. 6(a) show the sliding mode control input and sliding surfaces respectively. Fig. 6(b) shows the convergence of model states in short time and smoothly without shattering.

IV. CONCLUSION

Balancing an inverted pendulum in the presence of external disturbances and parametric uncertainty was crucial. The inverted pendulum was successfully balanced along to and from horizontal direction using a sliding mode-based control design. It was shown that the pendulum was stabilized. The sliding mode-based control design dealt with the modelling uncertainties and external disturbances very adequately. In addition, the control design of SMC guaranteed the system converges in a finite time. Further analysis and work was made to reduce the chattering that inherently comes along with the sliding mode as shown in the simulation results.

REFERENCES

[1] A. S. Al-Araji, "An adaptive swing-up sliding mode controller design for a real inverted pendulum system based on culture-bees algorithm," *European Journal of Control*, vol. 45, pp. 45–56, Jan. 2019.

[2] S. Jadlovska and J. Samovský, "Classical double inverted pendulum — A complex overview of a system," *Proceedings of IEEE 10th*

International Symposium on Applied Machine intelligence and informatics (SAMi), pp. 103–108, Jan. 2012.

[3] S. Wenxia and C. Wei, "Simulation and debugging of LQR control for two-wheeled self-balanced robot," *Proceedings of Chinese Automation Congress (CAC)*, pp. 2391–2395, Oct. 2017.

[4] F. Dai, X. Gao, S. Jiang, W. Guo, and Y. Liu, "A two-wheeled inverted pendulum robot with friction compensation," *Mechatronics*, vol. 30, pp. 116–125, Sep. 2015.

[5] H. G. Nguyen, J. Morrell, K. D. Mullens, A. B. Burmeister, S. Miles, N. Farrington, K. M. Thomas, and D. W. Gage, "Segway robotic mobility platform," *Proceedings of SPIE*, vol. 5609, pp. 207–220, Dec. 2004.

[6] Y. Zhang, L. Zhang, W. Wang, Y. Li, and Q. Zhang, "Design and implementation of a two-wheel and hopping robot with a linkage mechanism," *IEEE Access*, vol. 6, pp. 42422–42430, 2018.

[7] Y. Sakagami, R. Watanabe, C. Aoyama, S. Matsunaga, N. Higaki, and K. Fujimura, "The intelligent ASIMO: System overview and integration," *Proceedings of IEEE/RSJ Int. Conf. Intell. Robots System*, pp. 2478–2483, Sep.–Oct. 2002.

[8] J. Chestnutt, M. Lau, G. Cheung, J. Kuffner, J. Hodgins, and T. Kanade, "Footstep planning for the honda ASIMO humanoid," *Proceedings of IEEE Int. Conf. Robot. Autom.*, pp. 629–634, Jan. 2006.

[9] M. Rosenblum and A. Pikovsky, "Synchronization: From pendulum clocks to chaotic lasers and chemical oscillators," *Contemp. Phys.*, vol. 44, no. 5, pp. 401–416, Sep. 2003.

[10] F. Dörfler and F. Bullo, "Synchronization in complex networks of phase oscillators: A survey," *Automatica*, vol. 50, no. 6, pp. 1539–1564, Jun. 2014.

[11] Inteco.com.pl. Pendulum & Cart Control System. Accessed: Nov. 22, 2019. [Online]. Available: <http://www.inteco.com.pl/>

[12] Feedback-instruments.com. Ball With Pendulum Suspension. Accessed: Nov. 22, 2019. [Online]. Available: <http://www.feedbackinstruments.com/>

[13] Quanser.com. Rotary Inverted Pendulum. Accessed: Nov. 22, 2019. [Online]. Available: <http://www.quanser.com/>

[14] J. K. Roberge, J. K., "1960 the mechanical seal," Bachelor's Thesis, Massachusetts Institute of Technology (MIT), 1960.

[15] J.-J. Wang, "Simulation studies of inverted pendulum based on PID controllers," *Simul. Model. Pract. Theory*, vol. 19, no. 1, pp. 440–449, Jan. 2011.

[16] L. B. Prasad, B. Tyagi, and H. O. Gupta, "Optimal control of nonlinear inverted pendulum dynamical system with disturbance input using PID controller and LQR," in *Proc. IEEE Int. Conf. Control Syst., Comput. Eng.*, Nov. 2011, pp. 540–545.

[17] C. Aguilar-Ibañez, J. A. Mendoza-Mendoza, M. S. Suarez-Castanon, and J. Davila, "A nonlinear robust PI controller for an uncertain system," *Int. J. Control*, vol. 87, no. 5, pp. 1094–1102, May 2014.

[18] S.A. Ajwad, J. Iqbal, M.I. Ullah, A. Mehmood, "A systematic review of current and emergent manipulator control approaches", *Front. Mech. Eng.* 10, 198–210, 2015.

[19] R. Toscano, "A simple robust PI/PID controller design via numerical optimization approach", *J. Process Control* 15, 81–88, 2005.

[20] Andrej Rybovic, Martin Pricinsky, Marek Paskala, "Control of the inverted pendulum using state feedback control," 2012 ELEKTRO, June 2012.

[21] M.I. Ullah, S.A. Ajwad, M. Irfan, J. Iqbal, "Non-linear control law for articulated serial manipulators: Simulation augmented hardware implementation", *Elektronika ir Elektrotehnika*, vol. 22, no. 1, pp. 3–7, 2016.